Reprinted from Macromolecules, 1985, 18, 1980.

Effects of Annealing and Prior History on Enthalpy Relaxation in Glassy Polymers. 5. Mathematical Modeling of Nonthermal Preaging Perturbations

I. M. Hodge*† and A. R. Berens

BFGoodrich Research and Development Center, Brecksville, Ohio 44141.
Received February 4, 1985

ABSTRACT: Computer simulation studies of the effects of hydrostatic pressure, tensile stress, and vapor-induced swelling on the physical aging of glass poly(vinyl chloride) (PVC) are presented. Published data indicate that application and rapid release of these nonthermal perturbations before aging produce glasses with elevated enthalpies and increased aging rates compared with those of unstressed glasses. These experimental observations are well described by a modified version of a phenomenological model which gives a good account of purely thermal history effects (Hodge, I. M.; Berens, A. R. *Macromolecules* **1982**, *15*, 762).

1. Introduction

In earlier papers of this series[1-4] it was shown that the effects of physical aging on enthalpy relaxation in polymers are described with good accuracy by a four-parameter phenomenological model based on the work of Tool,[5] Narayanaswamy,[6] Mazurin et al.,[7] and DeBolt et al.[8] This model reproduces the effects of cooling rate, aging time, aging temperature, and heating rate on the temperature and magnitude of heat capacity maxima observed in many aged polymers[2] and can be fitted to experimental data by standard optimization procedures.[3,4] In this paper we extend the model to include the effects on physical aging of hydrostatic pressure, tensile stress, and vapor-induced swelling, applied and released before aging. Our goal is to reproduce, qualitatively, experimental data with a calculation procedure which is computationally efficient and convenient.

We first review published experimental data that are relevant to our modeling studies. The effects of hydrostatic pressure on enthalpy relaxation in polymers have been studied experimentally by several investigators. Weitz and Wunderlich[9] observed isobaric heat capacity maxima in DSC scans, at 5 K min^{-1} and atmospheric pressure, of polystyrene (PS) and poly(methyl methacrylate) (PMMA) glasses formed by cooling at 5 K h^{-1} under hydrostatic pressures ranging from 0 to 345 MPa (0–3.45 kbar). At low pressure (69 MPa) the large heat capacity overshoot near T_g, characteristic of slowly cooled and rapidly heated glasses, was diminished compared with that of the glass formed at atmospheric pressure. At intermediate pressure (207 MPa) the heat capacity maximum moved to a lower temperature, T_{max}, to appear as a sub-T_g peak (magnitude $C_{p,max}$), similar to those observed by Illers[10] and others[1,11-13] in aged PVC glasses formed at atmospheric pressure. At the highest pressure (345 MPa) a broad exothermic heat capacity minimum developed between T_{max} and T_g. Similar results were observed by Yourtee and Cooper,[14] Dale and Rogers,[15] and Wetton and co-workers[16,17] for PS and by Kimmel and Uhlmann[18] and Price[19] for PMMA. For nonpolymeric glasses [phenolphthalein, sucrose, KNO_3/$Ca(NO_3)_2$] Weitz and Wunderlich observed only a decrease in overshoot near T_g with increasing pressure.[9] Prest and co-workers[12,13] reported heat capacity data obtained during heating at 20 K min^{-1} for PVC formed by cooling at 20 K min^{-1} under hydrostatic pressures ranging from 100 to 600 MPa and aged at room temperature and atmospheric pressure for 110 days. The sub-T_g heat capacity peak moved to slightly lower temperatures and became more asymmetric with increasing pressure. Berens and Hodge[1,11] observed that cold drawing, powder compaction, and vapor-induced swelling of glassy PVC accelerated the rate of sub-T_g peak development with aging time but noted that T_{max} was a weak function of the type and magnitude of the nonthermal perturbation. Similar findings were reported by Shultz and Young[20] for freeze-dried PS and PMMA and by Prest and Roberts[12] for mechanically compacted PS powder.

2. Modeling Studies

Before describing the introduction of nonthermal perturbations, we first review the model and calculation procedure described in detail elsewhere[2] for purely thermal histories.

2.1. Thermal Histories. The calculation procedure treats cooling and heating as a series of temperature steps and isothermal holds whose relative magnitudes are determined by the cooling and heating rates. Aging is introduced as an isothermal hold during cooling. The response of enthalpy to each temperature step is described by a response function $\phi(t)$, which for convenience and good accuracy is chosen to be of the form

$$\phi(t) = \exp[-(t/\tau_0)^\beta] \tag{1}$$

The ratio t/τ_0 is the reduced time

$$t_r = t/\tau_0 \tag{2}$$

The relaxation time τ_0 depends on temperature T and fictive temperature T_f according to the empirical Narayanaswamy expression[6]

$$\tau_0 = A \exp\left[\frac{x\Delta h^*}{RT} + \frac{(1-x)\Delta h^*}{RT_f}\right] \tag{3}$$

where x is a numerical measure of nonlinearity ($1 \geq x >$

† Present address: Research Laboratories, Eastman Kodak Co., Rochester, NY 14650.

0), Δh^* is an activation enthalpy that determines the cooling rate dependence of T_g,[21] and A and Δh^* together determine T_g:

$$\ln A \approx \ln \tau_0|_{T=T_g} - \Delta h^*/RT_g \quad (4)$$

By continually updating τ_0 as T_f relaxes in response to each temperature step, the nonlinearily is removed and the response to cooling, aging, and heating can be calculated by applying Boltzmann superposition. It is assumed that A, β, x, and Δh^* are independent of T and T_f.

The calculated heat capacity, dT_f/dT, corresponds to the experimental normalized heat capacity C_p^N, which has values of 0 and 1 in the glassy and liquid state, respectively.

2.2. Nonthermal Preaging Perturbations. 2.2.1. Hydrostatic Pressure. Pressure increases T_g and is introduced into the model by lengthening τ_0 in eqs 1 and 3. This can be accomplished in three ways, all of which produce similar results: either Δh^* or A can be increased or T_f decreased such that $T_f < T$ at equilibrium for $P > 0$. For the experimental protocols considered here changes in Δh^*, A, or T_f are applied during cooling from above T_g to the aging temperature and removed during aging and reheating. The magnitude of these changes as a function of pressure can be estimated, with sufficient accuracy for our qualitative purposes, from the enthalpy-based Ehrenfest relation

$$(\partial T/\partial P)_H = -T_g V_g \Delta\alpha/\Delta C_p \quad (5)$$

where $\Delta\alpha$ and ΔC_p are the changes in thermal expansivity and isobaric heat capacity and V_g is the volume at the glass transition temperature T_g. This relation has been shown to be reasonably accurate for polymers.[22] The constancy of H for the partial derivative in eq 5 corresponds to fixed enthalpic fictive temperature, and differentiation of eq 3 at constant T_f gives for $T \approx T_f \approx T_g$

$$d \ln \tau_0|_{T_f}^P = \frac{-x\Delta h^*}{RT^2} dT \approx \frac{x\Delta h^*}{RT_g} \frac{V_g\Delta\alpha}{\Delta C_p} dP \quad (6)$$

The corresponding changes in Δh^*, T_f, and A required to change $\ln \tau_0$ by this amount are

$$d(\Delta h^*)^P \approx \frac{x\Delta h^* V_g \Delta\alpha}{\Delta C_p} dP \quad (7)$$

$$dT_f^P \approx \left(\frac{-x}{1-x}\right)\frac{T_g V_g \Delta\alpha}{\Delta C_p} dP \quad (8)$$

$$d(\ln A)^P \approx \frac{x\Delta h^*}{RT_g} \frac{V_g\Delta\alpha}{\Delta C_p} dP \quad (9)$$

For $T \approx T_e < T_g$, where T_e is the aging temperature, the right-hand sides of eq 7–9 are multiplied by a factor of order $(T_g/T_e)^2$. It is assumed for simplicity that x and β are independent of pressure and that $d(\Delta h^*)^P$, dT_f^P, and $d(\ln A)^P$ are the same in both liquid and glassy states (i.e., $T_g/T_e \approx 1$).

In some cases the original procedure[2] of dividing the aging time into 10 logarithmically even intervals produced initial time increments that were too long compared with the relaxation time and gave changes in T_f that lay outside the linear range (>2 K). To avert this the aging time (in seconds) was divided into 10 logarithmically even divisions per decade. With this procedure changes in T_f never exceeded 2 K per time step, and the computation time did not increase excessively.

2.2.2. Vapor-Induced Swelling and Mechanical Stress. The increased volume and configurational entropy of vapor-swollen PVC are expected to shorten the average relaxation time, in qualitative accord with the well-known WLF and Adam–Gibbs expressions. For cold-drawn PVC film, dilation is expected to occur as a result of a Poisson ratio less than 0.5, again resulting in a shortened relaxation time (as discussed by Matsuoka[23]). Both perturbations can therefore be introduced into the calculation as a decrease in τ_0 immediately before aging. As in the calculation of hydrostatic pressure effects, the change in τ_0 can be effected by variation of Δh^*, A, or T_f with similar results. The calculation results presented here were obtained by varying T_f by an amount ΔT_f^s. The changes in τ_0 are assumed to occur instantaneously at the start of aging, this being justified by the rapid removal of stress and swelling perturbations (in seconds) compared with the aging times (a minimum of 1 h).[1,11] The change in τ_0 decays with reduced time during aging and reheating according to eq 1 and 2. For the case of ΔT_f^s

$$\Delta T_f^s(t_r) = \Delta T_f^s \exp[-(t_r - t_0)]^\beta \quad (10)$$

where ΔT_f^s is the instantaneous change in T_f before aging and t_0 is the elapsed reduced time at the start of aging. The response described by eq 10 is superimposed on the response to the thermal history, the two being coupled by their common dependence of τ_0 on T_f and T. The procedure is illustrated schematically in the inset of Figure 5.

The numerical changes in relaxation time induced by tensile stress and swelling are not as readily estimated as they are for hydrostatic pressure. Accordingly, values of ΔT_f^s in eq 10 were obtained empirically by matching the calculated and experimental values of $C_{p,max}^N$ for a fixed aging time (24 h in the present study), and the accuracy of the model is assessed by comparing the experimental and calculated values of $C_{p,max}^N$ and T_{max} at other aging times.

3. Results

3.1. Experimental Data. 3.1.1. Hydrostatic Pressure. Experimental heat capacity data for PVC obtained by Prest and Roberts[12] for three pressures are shown in Figure 1A in normalized form. Their highest pressure data are omitted since they were obtained on a sample that vitrified during pressurization before cooling.

3.1.2. Vapor-Induced Swelling and Tensile Stress. Experimental data of Berens and Hodge[11] on the effects of preaging exposure to varied pressures of CO_2 and CH_3Cl vapor on the DSC curves of aged PVC powder are shown in Figures 2 and 3. The particular pressures were chosen, by reference to independently determined sorption isotherms, to give approximately equal weight percent sorption of the two vapors: Curves A, B, C, and D in Figures 2 and 3 correspond to about 0, 1, 2, and 4 wt % sorption, respectively, of CO_2 and CH_3Cl (since CH_3Cl is more soluble, lower pressures were required to reach equal sorption). With both vapors, there is a progressive increase in the height of the DSC aging peak, and a small shift to lower T_{max}, with increasing vapor pressure. The similarity of the two sets of curves clearly suggests that aging is affected by the extent of sorption or dilation of the polymer, and not by the vapor pressure per se. A summary of the experimental values of $C_{p,max}^N$ and T_{max} as a function of vapor pressure is given in Table I.

DSC curves for PVC sheet samples aged after application and release of tensile stresses, also obtained by Berens and Hodge,[11] are shown in Figure 4. Preaging tensile stress up to 75% of the yield stress produced little effect on enthalpy relaxation (curves A and B), but stressing to and beyond the yield point (curves C and D) caused a

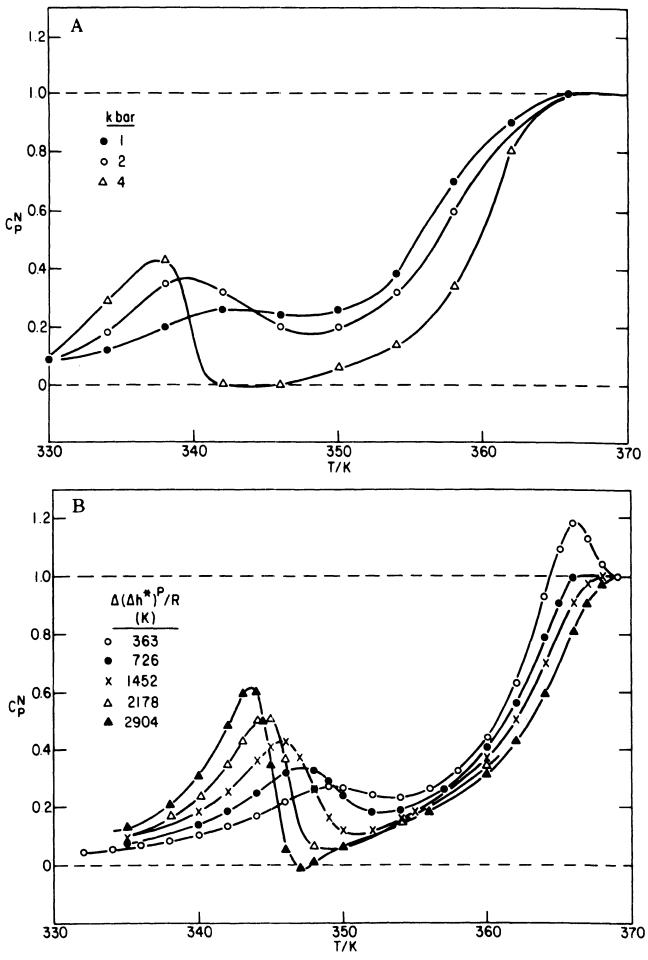

Figure 1. (A) Normalized experimental heat capacities of PVC, after cooling at 20 K min^{-1} at the indicated hydrostatic pressures and aging at room temperature and pressure for 110 days. Heating rate 20 K min^{-1} at atmospheric pressure. Raw heat capacity data from Prest and Roberts.[12] (B) Calculated normalized heat capacities of PVC for the indicated values of $\Delta(\Delta h^*)^P$ (see section 2.2.1 of text) and the same thermal history as in (A). Unperturbed parameters were ln A (s) = −619.0, $\Delta h^*/R = 225 \times 10^3$ K, x = 0.11, and β = 0.25.

Table I
Observed and Calculated Effects of Preaging Perturbations (after Aging 24 h at 313 K)

		T_{max}, K		$C_{p,max}{}^N$	
exptl perturbation	$\Delta T_f{}^s$	exptl (±1 K)	calcd (±1 K)	exptl (±0.02)	calcd (±0.01)
P_{CO_2}, MPa					
0	0	347 (sh)[a]	346	0.16	0.18
0.76	0	346	346	0.15	0.18
1.52	1	345	344	0.20	0.21
3.44	2	343	343	0.22	0.24
P_{CH_3Cl}, MPa					
0	0	347 (sh)	346	0.16	0.18
0.041	0.5	346	345	0.19	0.19
0.096	1	344	344	0.22	0.21
0.172	2	343	343	0.24	0.24
tensile stress, MPa					
0	0	347 (sh)	346	0.16	0.18
46	3	340	342	0.23 (±0.04)	0.28

[a] Shoulder.

pronounced DSC aging peak. Curve D for the material stressed beyond the yield point also exhibits a strong exotherm and shift in T_g. These are thought to be due to release of energy stored as orientation.[11] Values of $C_{p,max}{}^N$ and T_{max} corresponding to curve C in Figure 4 are also

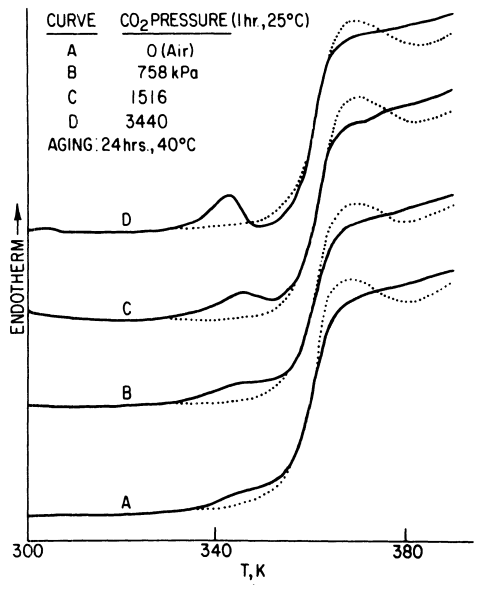

Figure 2. DSC curves for free-cooled PVC powder, after preaging exposure to CO_2 at the indicated vapor pressure for 1 h at 25 °C, and after aging for 24 h at 40 °C.[11]

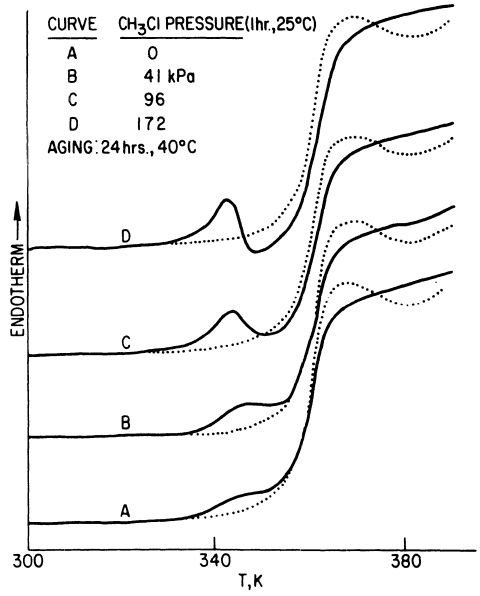

Figure 3. DSC curves for free-cooled PVC powder, after preaging exposure to CH_3Cl at the indicated vapor pressures for 1 h at 25 °C, and after aging for 24 h at 40 °C.[11]

included in Table I. A summary of earlier experimental results obtained by Berens and Hodge for PVC[1] are reproduced in Figure 5 in the form of $C_{p,max}{}^N$ and T_{max} vs. aging time, for the indicated thermal and nonthermal preaging histories. In these studies the tensile stress history of the films[1,11] consisted of cold drawing to just above the yield point (about 100% elongation) in an Instron, followed by stress removal immediately before aging at 40 °C.

3.2. Calculation Results. 3.2.1. Preaging Hydrostatic Pressure. Insertion of the experimental values of ΔC_p, $\Delta\alpha$, V_g, and T_g for PVC into eq 7–9 [ΔC_p = 0.10 cal K^{-1} g^{-1},[24] $\Delta\alpha \approx 2 \times 10^{-4}$ K^{-1},[22] V_g = 0.7 cm^3 g^{-1}, T_g = 363 K,[2], x = 0.11,[2] $\Delta h^*/R = 225 \times 10^3$ K^2] gives $\Delta(\Delta h^*)^P/R\Delta P \approx 8.4$ K MPa^{-1}, $\Delta T_f{}^P/\Delta P \approx 0.015$ K MPa^{-1} and $\Delta(\ln A)^P/\Delta P \approx 0.023$ MPa^{-1}. Calculated values of $C_{p,max}{}^N$ and T_{max} for equivalent changes in T_f, Δh^*, and ln A for PVC are listed in Table II. Almost identical results are obtained for each calculation procedure. Calculated nor-

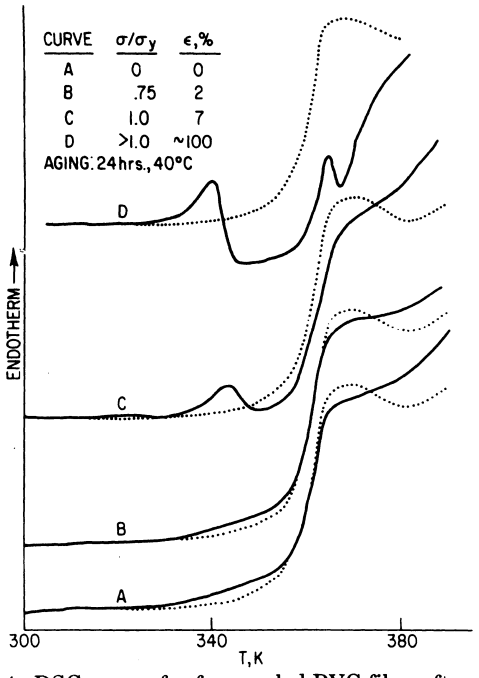

Figure 4. DSC curves for free-cooled PVC film, after preaging tensile stresses were applied for 10 min (curves A, B, and C), and after aging 24 h at 40 °C. Yield stress (σ_y) is about 46 MPa. Curve D is for film cold drawn to 100% elongation at 1% min^{-1}.[11]

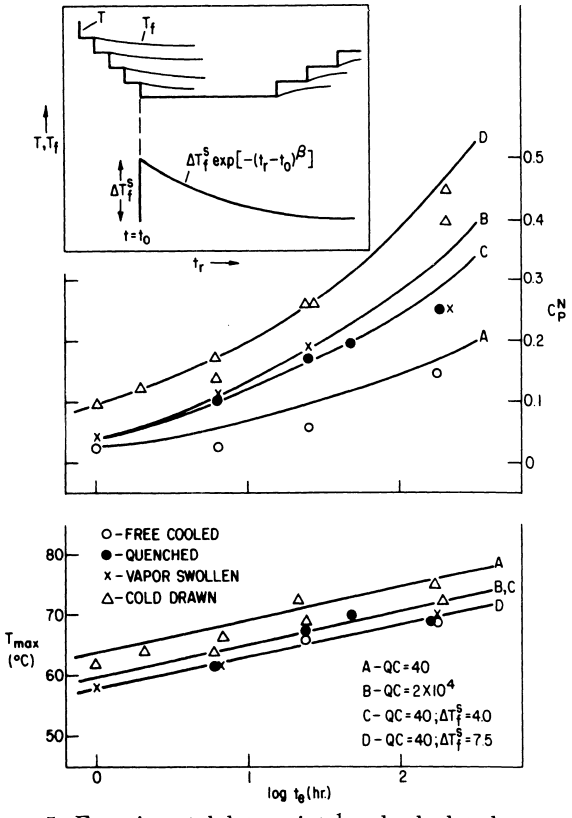

Figure 5. Experimental data points[1] and calculated curves for the aging time dependences of $C_{p,max}{}^N$ and T_{max} for PVC for the indicated thermal and nonthermal histories. Inset: Schematic of the calculation procedure (see section 2.2.2 of text).

malized heat capacities, using atmospheric pressure parameters for PVC obtained from purely thermal histories,[2] are shown in Figure 1B for the indicated values of $\Delta(\Delta h^*)^P$. The experimentally observed sharpening and increased asymmetry of the sub-T_g heat capacity peaks with pressure, the modest decrease in T_{max}, and the increase in T_g are all reproduced by the calculation.

Table II
Calculated $C_{p,max}$ and T_{max} for Parameter Increments Q_C = 20 K min^{-1}, Q_H = 20 K min^{-1}, t_e = 24 h, and T_e = 313 K

hydrostatic pressure, MPa	parameter increments		$C_{p,max}$	T_{max}, K
0	$-\Delta T_f^P$ (K)	0	0.167	347
100		1.52	0.205	344
200		3.04	0.251	342
400		6.08	0.350	340
600		9.12	0.460	339
0	Δln A	0	0.167	347
100		2.32	0.205	344
200		4.65	0.251	342
400		9.30	0.353	340
600		13.94	0.465	339
0	$\Delta(\Delta h^*/R)$ (K)	0	0.167	347
100		844	0.205	344
200		1689	0.249	342
400		3377	0.346	340
600		5066	0.455	339

3.2.2. Preaging Tensile Stress and Vapor-Induced Swelling. The calculated dependences of $C_{p,max}{}^N$ and T_{max} on aging time, using ΔT_f^s to change ln τ_0, are shown as solid lines in Figure 5. As stated in section 2.2.2 the value of ΔT_f^s for the perturbed glasses was determined from $C_{p,max}{}^N$ for an aging time of 24 h. For the unperturbed glasses no adjustable parameter was introduced, and the deviations between experimental and calculated curves in this case are due in part to the relatively large experimental uncertainties in $C_{p,max}{}^N$ and T_{max} for small sub-T_g peaks and to uncertainty in the (uncontrolled) cooling rate. The unperturbed parameters for PVC were those used in the hydrostatic pressure calculations, i.e., those obtained from analysis of purely thermal histories.[2] The calculated values of T_{max} and $C_{p,max}{}^N$ as a function of ΔT_f^s are compared with experimental values in Table I. There is excellent agreement between the calculated and experimentally observed relations between T_{max} and $C_{p,max}{}^N$.

4. Discussion

The ability of the mathematical model to reproduce the effects of hydrostatic pressure, vapor-induced swelling, and tensile stress, as well as thermal history, on subsequent enthalpy relaxation in PVC supports our previous suggestion[11] that the nonthermal preaging treatments may all be regarded as a generalized stress whose release increases the enthalpy of the glass. This results in the glass being further from equilibrium at the start of aging, and thus losing enthalpy more rapidly than an unstressed material.

The overall agreement between calculated and experimental results for the effects of hydrostatic pressure, tensile stress, and vapor-induced swelling on the physical aging of PVC indicates that the calculation procedures are essentially correct. In particular, the assumption that these nonthermal perturbations change only the relaxation time appears to be valid. Any changes in the shape parameter β with T or T_f are evidently of minor importance, but it is not clear from the present results whether this is due to the changes being numerically very small or if the calculated results are simply insensitive to them (variation of β with T or T_f would require a different calculation procedure and was not attempted). Recently published theoretical results,[25-28] which predict that small changes in β with T_f produce large changes in τ_0, suggest the former is more likely; evidently the effects of nonlinearity are much more important than those of changing β.

The experimental data shown in Figure 5 indicate that T_{max} increases appproximately linearly with log t_e, with a slope (about 5 K $decade^{-1}$) that is independent of history.